DOI 10.1007/s10812-019-00793-6
Journal of Applied Spectroscopy, Vol. 86, No. 1, March, 2019 (Russian Original Vol. 86, No. 1, January–February, 2019)

SPECTRAL ELLIPSOMETRY STUDY OF SILICON SURFACES IMPLANTED WITH OXYGEN AND HELIUM IONS

V. V. Bazarov,*[*] V. I. Nuzhdin, V. F. Valeev, and N. M. Lyadov UDC 543.42:546.28

Results are given for a spectral ellipsometry study of silicon surfaces implanted with oxygen ions in the dose range $7.5 \cdot 10^{14}$–$3.7 \cdot 10^{16}$ ions/cm^2 and helium ions in the range $6 \cdot 10^{16}$–$6 \cdot 10^{17}$ ions/cm^2 with energy 40 keV at constant ion current density 2 μA/cm^2. The irradiated substrates were at room temperature. Curves are shown for the dependence of the thickness of the implanted layer in the irradiated plates and the dependence of the extent of amorphization of this layer on the ion implantation dose.

Keywords: *amorphous silicon, ion implantation, spectral ellipsometry.*

Ion implantation is one of the most commonly used methods for the controlled change of the surface properties of semiconductor materials. Low-energy high-dose ion implantation in silicon is accompanied by its amorphization, which begins almost immediately after the onset of implantation. Various workers [1–7 and the references presented] have already shown that for monocrystalline silicon (*c*-Si) implanted with various types of ions in a broad energy range, spectral ellipsometry (SE) is an informative method for studying partially amorphized semiconductor layers. This method is rather efficient in practice since the optical constants of α-Si and *c*-Si differ considerably in the visible wavelength range.

Rutherford backscattering spectroscopy (RBS) is commonly used for the experimental description of the concentration of radiation defects generated upon ion implantation and evaluation of the depth distribution of these defects [8, 9]. However, the depth of penetration of ions with energies about 40 keV is only tens of nanometers. Thus, RBS provides little information on such thin layers. An exception is found for high-resolution RBS [10, 11] but this specific method is difficult to realize in practice.

In the present work, results are given for a spectral ellipsometry study of the stepwise amorphization of *c*-Si upon its implantation with high doses of low-energy O^+ and He^+ ions (40 keV) .

The samples selected for the SE experiments were monocrystalline *c*-Si substrates with orientation (100) implanted with $^{16}O^+$ ions in the dose range $D = 7.5 \cdot 10^{14}$–$3.7 \cdot 10^{16}$ ions/cm^2 and $^4He^+$ ions in the dose range $1 \cdot 10^{17}$–$6 \cdot 10^{17}$ ions/cm^2 with energy $E = 40$ keV and current density in the ion beam 1–2 μA/cm^2. The implantation was carried out using an ILU-3 ion accelerator at residual vacuum 10^{-5} torr.

Optical analysis of the implanted silicon layers was carried out using an ES-2 spectroscopic ellipsometer with binary polarization modulation at wavelengths 380–820 nm (spectral resolution 6 nm, measurement step 10 nm, light beam incidence angle $\Psi = 70^o$). The ES-2 ellipsometer has been described by Khomich et al. [12]. The electron microscopy images were obtained on a high-resolution Carl Zeiss EVO 50XVP scanning electron microscope.

An optical model of an isotropic homogeneous thin layer consisting of a mixture of crystalline (*c*-Si) and amorphous phases (α-Si) on a monocrystalline substrate of *c*-Si was selected for analysis of the experimental spectral curves of samples implanted with O^+ ions. The thickness of the implanted layer (d_{exp}) and content of the amorphous α-Si phase in the implanted layer (occupancy factor f and thickness of the layer of natural oxide SiO_2 on the sample surface d_{SiO2}) served as the fitting parameters in the framework of this model. The determination of the optical constants (refraction index n and extinction coefficient k) of the implanted layer relative to the content of the α-Si phase was carried out in accord with the Bruggerman effective medium approximation. The calculated ellipsometric angles spectra $\Psi_{th}(\lambda)$ and $\Delta_{th}(\lambda)$ obtained by variation of the

[*]To whom correspondence should be addressed.

Kazan E. K. Zavoisky Physical-Technical Institute (KPhTI), Kazan Science Center, Russian Academy of Sciences, 107 Sibirskii Trakt, 420029, Russia; email: vbazarov@gmail.com, nuzhdin@kfti.knc.ru, valeev@kfti.knc.ru, nik061287@mail.ru. Translated from Zhurnal Prikladnoi Spektroskopii, Vol. 86, No. 1, pp. 151–154, January–February, 2019. Original article submitted June 26, 2018.

 0021-9037/19/8601-0134 ©2019 Springer Science+Business Media, LLC

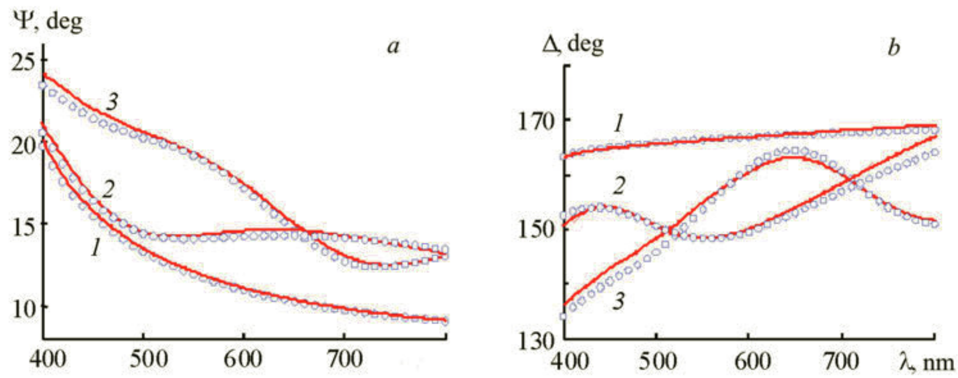

Fig. 1. Experimental (points) and calculated ellipsometric angles spectra (lines) Ψ(λ) (a) and Δ(λ) (b) for a nonirradiated sample (1) and samples implanted with O^+ ion doses of $7.5\cdot10^{14}$ (2) and $7.5\cdot10^{15}$ ions/cm^2 (3).

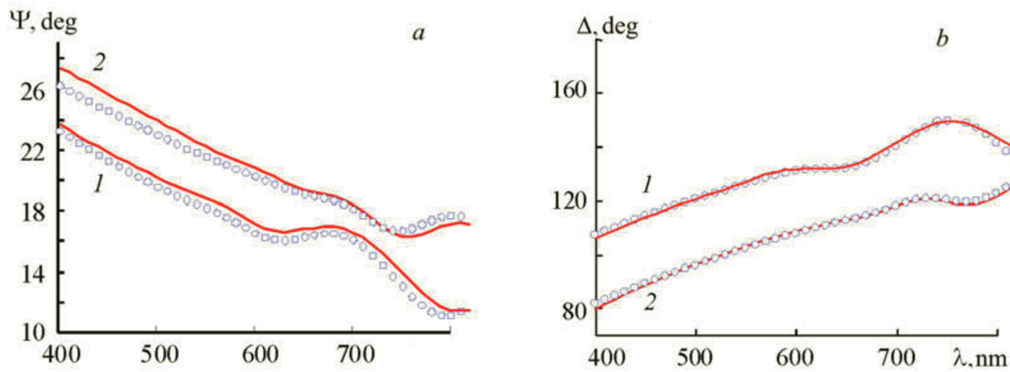

Fig. 2. Measured (points) and calculated ellipsometric angles spectra (lines) Ψ(λ) (a) and Δ(λ) (b) for samples implanted with He^+ ions by doses of $3\cdot10^{17}$ (1) and $6\cdot10^{17}$ ions/cm^2 (2).

variables d_{exp}, d_{SiO2}, and f were compared with the experimental spectra $\Psi_{th}(\lambda)$ and $\Delta_{exp}(\lambda)$ in order to obtain the best fit. Figure 1 gives the ellipsometric angles spectra for the nonirradiated sample and two samples implanted with O^+ ions (doses $7.5\cdot10^{14}$ and $7.5\cdot10^{15}$ ions/cm^2).

For all the samples implanted with O^+ ions, $d_{SiO2} \approx 1$–4 nm. Analysis of the curves for samples implanted with He^+ ions show that satisfactory accord of the experimental and calculated ellipsometric angles spectra can be achieved only for large implantation doses when the surface region is almost entirely amorphized. Thus, the thickness of the amorphized layer (d_{exp}) and thickness of the surface layer containing a mixture of natural SiO_2 and the amorphous silica phase (d_{SiO2}) were taken as the fitting parameters of the model. The surface layer with thickness ~30 nm was found to consist of ~30% SiO_2 and ~70% α-Si.

For initial evaluation of the thickness of the implanted layer, calculations were carried out using the SRIM-2011 program for computer modelling of ion stopping in matter [13]. The modelling showed that in the initial irradiation period, the oxygen atoms accumulated near the Si surface with maximum of the Gauss statistical distribution at depth R_p ~ 100 nm and meansquare deviation Δ_{Rp} ~ 38 nm. In the case of implanted He^+ ions, R_p ~ 353 nm, Δ_{Rp} ~ 97 nm.

Our SE study of silicon amorphization upon the implantation of O^+ ions with energy 40 keV in the dose range $7.5\cdot10^{14}$–$3.7\cdot10^{16}$ ions/cm^2 (Fig. 2a) showed that for implantation dose $7.5\cdot10^{14}$ ions/cm^2, a partially amorphized layer with thickness ~50 nm is formed on the silicon surface with 40% amorphous phase. Increasing the irradiation dose to $3.7\cdot10^{16}$ ions/cm^2 leads to a steady increase in the thickness of this layer to ~100 nm.

The results for silicon plates implanted with helium ions by doses of $3.1\cdot10^{17}$ and $6.2\cdot10^{17}$ ions/cm^2 are shown in Fig. 3b. The first signs of amorphization appear at implantation dose $6\cdot10^{16}$ ions/cm^2. Complete amorphization does not occur even at rather high implantation dose $1\cdot10^{17}$ ions/cm^2.

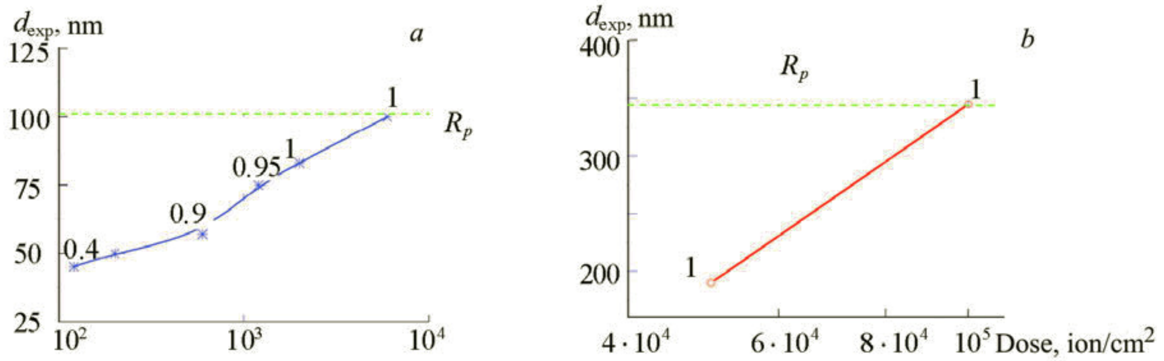

Fig. 3. Dependence of the thickness of the implanted layer (d) of silicon on the O^+ (a) and He^+ ion implantation dose (b) with energy 40 keV from the SE data. The content of the amorphous silicon phase in the implanted layer determined by modelling of the SE spectra is shown.

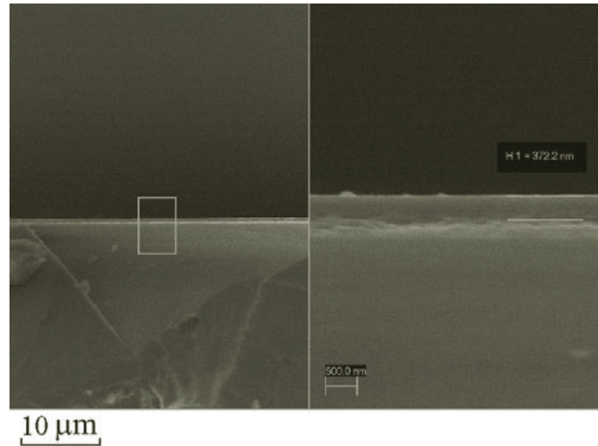

Fig. 4. Electron microscopy images of a chip of a silicon plate irradiated with He^+ ions. The dose was $6{\cdot}10^{17}$ ions/cm^2.

In order to explain why the calculated values R_p are greater than the experimental thickness of the amorphized layer, we must take account of the following circumstances. The masses of the incident $^4He^+$ and $^{16}O^+$ ions are significantly lower than the mass of the ^{28}Si atom. In this case, the disordered layer is formed through a homogeneous mechanism as a result of the gradual accumulation of point defects over the entire surface region with nonuniform close-to-Gaussian distribution over the depth. In this case, as shown by Ziegler et al. [13 and references presented], the maximum energy losses (energy release function) is located at a depth of $0.8R_p$. Thus, the maximum content of the amorphous phase should be found at this depth. We note that the use of rectangular angle distribution of defect concentration over the depth instead of a Gaussian distribution in the SE calculations gives rather good agreement with the calculations using the SRIM algorithm. A close-to-rectangular depth distribution of structural defects upon the implantation of PF_4^+ ions into silicon was described by Karabeshkin et al. [9] and supported in a SEM study of the implanted samples.

Figure 4 shows that the thickness of the light film (presumably, the amorphized layer) corresponds approximately to the thickness of the implanted layer obtained from the SE study. There is no such layer on the other side of the sample.

Thus, the SE method was used for structural analysis of the silicon surface layers implanted with light ions (O^+ and He^+). For implantation dose $7.5{\cdot}10^{14}$ ions/cm^2, a partially amorphized layer with thickness ~50 nm was formed on the silicon surface. With a further increase in the irradiation dose to $3.7{\cdot}10^{16}$ ions/cm^2, we find a completely amorphized layer and a steady increase in its thickness to ~100 nm. In the case of high-dosage implantation of He^+ ions, the spectral ellipsometry method also permits evaluation of the thickness of the implanted layer. These examples demonstrate the efficiency of using spectral ellipsometry for characterizing implanted samples.

REFERENCES

1. P. Petrik, O. Polga, M. Fried, T. Lohner, N. Q. Khanh, and J. Gyulai, *J. Appl. Phys.*, **93**, 1987–1990 (2003).
2. D. Shamiryan and D. V. Likhachev, in: M. Goorsky (editor), *Ion Implantation*, InTech (2012), pp. 89–104.
3. V. V. Bazarov, V. F. Valeev, V. I. Nuzhdin, Y. N. Osin, G. G. Gumarov, and A. L. Stepanov, *Solid State Phenom.*, **233–234**, 525–529 (2015).
4. V. V. Bazarov, V. I. Nuzhdin, V. F. Valeev, V. V. Vorobev, Yu. N. Osin, and A. L. Stepanov, *Zh. Prikl. Spektrosk.*, **83**, No. 1, 55–59 (2016) [*J. Appl. Spectrosc.*, **83**, 47–50 (2016)].
5. V. V. Bazarov, V. I. Nuzhdin, V. F. Valeev, and A. L. Stepanov, *Vacuum*, **148**, 254–257 (2018).
6. K. Tsunoda, S. Adachi, and M. Takahashi, *J. Appl. Phys.*, **91**, 2936–2941 (2002).
7. K. Kurihara, S. Hikino, and S. Adachi, *J. Appl. Phys.*, **96**, 3247–3254 (2004).
8. K. V. Karabeshkin, P. A. Karasev, and A. I. Titov, *Fiz. Tekhn. Poluprovodn.*, **47**, No. 2, 206–210 (2013) [*Semiconductors*, **47**, 242–246 (2013)]
9. K. V. Karabeshkin, P. A. Karasev, and A. I. Titov, *Fiz. Tekhn. Poluprovodn.*, **50**, No. 8, 1009–1015 (2016) [*Semiconductors*, **50**, No. 8, 989–995 (2016)].
10. K. Kimura, Y. Oota, K. Nakajima, M. Suzuki, T. Aoki, J. Matsuo, A. Agarwal, B. Freer, A. Stevenson, and M. Ameen, *Nucl. Instr. Methods Phys. Res. B*, **211**, 206–210 (2003).
11. K. Kimura, S. Joumori, Y. Oota, K. Nakajima, and M. Suzuki, *Nucl. Instr. Methods Phys. Res. B*, **219–220**, 351–357 (2004).
12. A. V. Khomich, V. I. Kovalev, E. V. Zavedeev, R. A. Khmelnitskiy, and A. A. Gippius, *Vacuum*, **78**, 583–587 (2005).
13. J. F. Ziegler, J. P. Biersack, and M. D. Ziegler, *SRIM. The Stopping and Range of Ions in Matter*, SRIM Company (2008).